



## Clinical and imaging features in surgically verified patients over 11 years and literature review

Rajanikanth Rao Vedula<sup>1\*</sup>, Yadagiri Kummary<sup>1</sup>, Sunil Reddy Gurram<sup>1</sup>, Anantram Gudipati<sup>1</sup>, Sandeep Ponnaganti<sup>1</sup>, and Manas Kumar Panigrahi<sup>2</sup>

<sup>1</sup>Department of Radiology, Krishna Institute of Medical Sciences, Minister Road, Secunderabad-500003, Telangana, India

<sup>2</sup>Department of Neurosurgery, Krishna Institute of Medical Sciences, Minister Road, Secunderabad-500003, Telangana, India

### Abstract

**Background:** Controversy continues in the treatment decisions despite advanced imaging techniques. Though specific diagnosis by imaging is not precise. Diffusion weighted imaging is useful in a small proportion of patients. We evaluated the features of magnetic resonance imaging (MRI) with histopathological findings in patients with lesions of the cavernous sinus (CS).

**Materials and methods:** Retrospective analysis of clinical, imaging and histopathological findings of lesions involving cavernous sinus (CS) in 27 consecutive patients was done.

**Results:** The average age of the study population was  $41.12 \pm 14.49$  (13-63) years; with 16 (59.2%) males. Visual disturbances were the most common complaints, reported in 62.0% and cranial nerve involvement was observed in 55 % of the patients. Complete excision was done in nine (33.3%) patients. Post-operative histopathology revealed meningiomas and hemangiomas in six (22.2%) patients each. While, five (18.5%) patients had schwannoma; fungal granuloma was observed in three (11.1%). Imaging based diagnosis showed concordance with histopathology in five (85.0%) patients with hemangioma. Among fungal granuloma, schwannoma and meningiomas, the concordance was 66.6%, 40.0% and 33.3% respectively. In the entire study population, concordance was 44.4%.

**Conclusions:** MR signal intensities are similar in neoplasms, infections, vascular lesions and inflammatory lesions. Cavernous hemangiomas are most often mistaken for other lesions but may be characterized by intense contrast enhancement and absence of restriction of DWI and blooming on GRE sequence. In lesions of cavernous sinus, accuracy of diagnosis on MRI is less than 50%. Diagnosis on MRI is more accurate in hemangiomas and fungal granulomas. Non-invasive diagnosis of granulomatous lesions may help plan appropriate management strategy.

**Keywords:** cavernous sinus; magnetic resonance imaging; diffusion weighted imaging

### Keymessage

While other benign neoplastic lesions in cavernous sinus exhibit non-specific appearances, hemangiomas demonstrate consistent features on imaging. MRI has a valuable role in the follow-up of granulomatous and inflammatory lesions.

### Introduction

The cavernous sinus (CS) is an intracranial dural venous sinus extending from the orbital apex and superior orbital fissure anteriorly, to the Meckel's cave posteriorly. It is composed of a network of small venous channels that may arbitrarily be divided into different compartments. The main venous influx into the CS is the superior and inferior ophthalmic veins, pterygoid

plexus, and sylvian vein and posteriorly into the superior and inferior petrosal sinuses. The internal carotid artery

**\*Corresponding author:** Rao RK Vedula, MD, DMRD, FRCP (Glasgow), Emeritus Professor, Krishna Institute of Medical Sciences, Minister Road, Secunderabad-500003, Telangana, India. Mobile: +91 9989773473; Email: [vedula@gmail.com](mailto:vedula@gmail.com)

Received 25 January 2022; Revised 14 March 2022; Accepted 22 March 2022; Published 30 March 2022

**Citation:** Vedula RR, Kummary Y, Gurram SR, Gudipati A, Ponnaganti S, Panigrahi MK. Clinical and imaging features in surgically verified patients over 11 years and literature review. J Med Sci Res. 2022; 10(2):47-59. DOI: <http://dx.doi.org/10.17727/JMSR.2022/10-11>

**Copyright:** © 2022 Vedula RR et al. Published by KIMS Foundation and Research Center. This is an open-access article distributed under the terms of the Creative Commons Attribution License, which permits unrestricted use, distribution, and reproduction in any medium, provided the original author and source are credited.

(ICA) is the most medial structure within the CS located in the carotid trigone. Cranial nerves III and IV and the first and second divisions of the cranial nerve V (from superior to inferior) are situated in the lateral dural wall of the CS (Figures 1 & 2). Sixth cranial nerve courses in the central part of the CS inferolateral to the ICA. These structures are involved by neoplastic, vascular, infective and infiltrative lesions. Neurogenic tumors, meningiomas, epidermoids, dermoids and cavernous hemangiomas commonly involve the cavernous sinus [1]. Patients present with oculomotor paresis, diplopia, sensory motor disturbances of facial muscles and rarely with symptoms and signs of cavernous sinus thrombosis by spread through the skull base and foramina (Figure 3). The two classifications based on anatomical location by Ishikawa and Jefferson demonstrated inflammatory lesions more in the anterior type and tumors were occupying mainly the posterior and the whole types. T2 hypointense signal pattern is noted in chronic inflammatory lesions, granulomas and lymphomas while cavernomas and hemangiomas demonstrate hyperintensity on T2 sequence. T1 hyperintensity is typically observed in dermoids, adenomas, melanomas and hemorrhagic lesions (Figure 4). Extradural transcavernous or intradural surgical approaches are decided depending on the plane of the lesion and its extent of location. Though primary radiation is offered as an option, many lesions require biopsy for specific treatment. We retrospectively reviewed the medical records for clinical, imaging and histological diagnostic findings of lesions involving CS. The tumor site, size, morphology or signal characteristics and post intravenous (I.V) gadodiamide enhancement pattern were assessed. The present case series of twenty seven patients describes the clinical presentation and MRI features correlating with histopathology that helped selection of treatment modality.

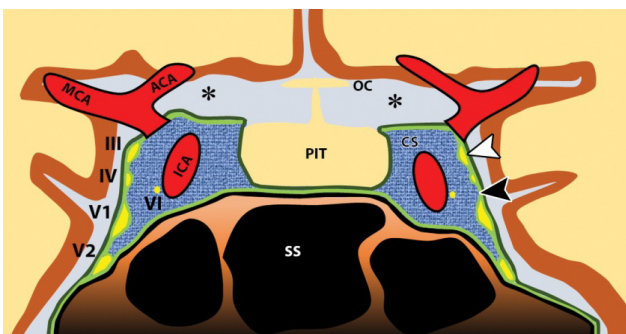


**Figure 1:** Diagram of a coronal section through the cavernous sinuses and the sella turcica. Note that the medial wall of the cavernous sinus (CS) is constituted by only a single layer of the dura mater. ACA = anterior cerebral artery, ICA = cavernous segment of the ICA, III = oculomotor nerve, IV = trochlear nerve, MCA = middle cerebral artery, OC = optic chiasm, PIT = pituitary gland, SS = sphenoid sinus, VI = abducens nerve, V1 = ophthalmic nerve, V2 = maxillary nerve, black arrowhead = inner periosteal layer of the dura, white arrowhead = outer meningeal layer of the dura, \* = subarachnoid.

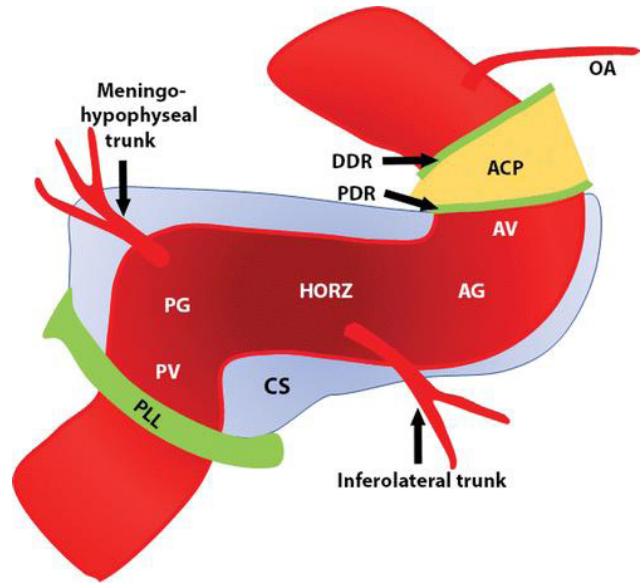


**Figure 2:** Diagram of the segments and major branches of the cavernous segment of the ICA. Light blue structure represents the cavernous sinus (CS). The segments of the cavernous carotid artery from proximal to distal are the posterior vertical (PV), the posterior genu (PG), the horizontal (HORZ), the anterior genu (AG), and the anterior vertical (AV). ACP = anterior clinoid process, DDR = distal dural ring, OA = ophthalmic artery, PDR = proximal dural ring, PLL = petrolingual ligament.

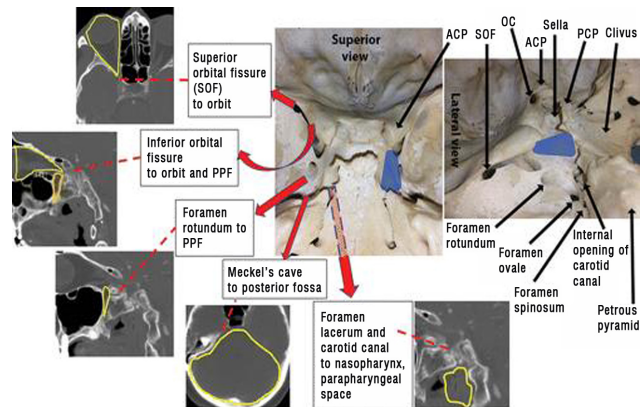


**Figure 3:** Anatomic pathways related to the cavernous sinuses and the regional bone anatomy. Blue areas represent the position of the cavernous sinuses in the floor of the middle cranial fossa. Yellow lines outline the anatomic region set in boldface in each label. ACP = anterior clinoid process, OC = optic canal, PCP = posterior clinoid process, PPF = pterygopalatine fossa (outlined in orange on image at far left).

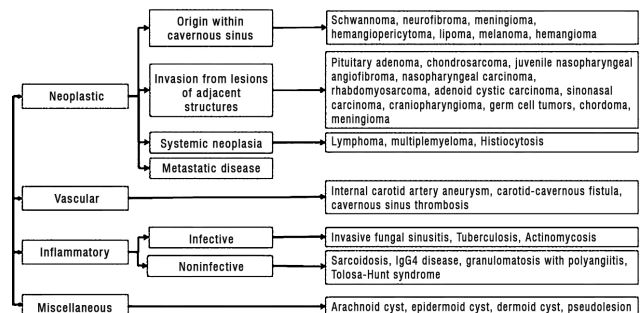


**Figure 4:** Etiologic classification of cavernous sinus lesions. IgG4 = immunoglobulin G4.

## Materials and methods

This retrospective study of data was approved by the hospital internal review board. Of the total 27 patients presenting with lesions in the cavernous sinus, 26 consecutive patients with CS lesions underwent MRI examination between 2008 and 2019 (age range, 13-63 years; mean age 41.12, SD  $\pm$  14.49; 16 males, 11 females with female to male ratio of 0.60). Both 1.5-T and 3-T systems were used for MR imaging. The imaging technique included conventional spin-echo, echo-planar diffusion-weighted imaging (DWI) and FLAIR sequence. DW images in 21 patients and GRE sequence in 24 were available. Axial T1-weighted (T1-W) contrast enhancement with Omniscan (Gadodiamide, GE Healthcare, Oslo, Norway) was supplemented with and without fat suppression pulse in addition to post contrast SPGR sequence.

## Technical parameters

(a) Spin-echo T1-W imaging: repetition time msec/echo time msec, 2000/20; inversion time 400, flip angle 90°; and matrix 296  $\times$  205; (b) Fast spin echo T2-weighted imaging (T2-W): 3000/90; flip angle 90°; and matrix 492  $\times$  479 for; and (c) Fluid-attenuated inversion recovery imaging: 10,000/125; 90°; and matrix, 300  $\times$  205. Other parameters: Slice gap was 1.5-2 mm with a 5-mm section thickness, and FOV 230  $\times$  250 mm. Echo-planar DW MR imaging was performed in the axial plane before contrast enhancement. T1-W 3 D spin-echo sequences without fat suppression and post contrast SPGR sequences were obtained using a matrix of 492  $\times$  479; slice thickness 1mm without slice gap; flip angle, 9°; repetition time/echo time 5/10 msec and FOV 240  $\times$  240. Intravenous dose of gadodiamide was 0.2 mL/kg (0.1 mmol/kg) body weight. T1-W, T2-FSE and FLAIR signal intensities were tabulated as hyper, hypo, iso intensities. Blooming and restriction of diffusion on

the GRE and DWI sequences and intensity of contrast enhancement on T1- fat suppressed sequences were evaluated. Two patients underwent digital subtraction angiography. Histopathological diagnosis of lesion in the cavernous sinus was verified from the notes in the medical case files retrospectively.

## Results

The study includes 27 patients and 59% were males. Visual disturbances were the predominant feature (62%) and about two thirds of the patients had no visual symptoms despite large size of the lesion. Cranial nerve involvement was observed in 55 % of the patients (Tables 1). Extra cavernous sinus involvement of Meckel's cave, cerebral peduncles and basal cisterns were seen in all except one. Of the 26 patients who received surgery, complete excision in 9 patients was possible and subtotal excision or biopsy in the others. Trace images of DWI demonstrated facilitated diffusion in 11 and restricted (hyperintense in DWI and hypointense in ADC) in 10 patients. Mean ADC value in 17 patients was 0.09176, wherein lesions with restricted diffusion showed 0.7914 and those with facilitated demonstrated 0.776  $\times$  10<sup>-3</sup> mm<sup>2</sup>/s. Apart from meningioma and schwannoma, blooming on GRE sequence was observed in pituitary tumour and an epidermoid cyst. Varying patterns of enhancement of the lesions were noted following intravenous contrast enhancement (Table 2&3). Follow up MRI examination of cavernous hemangiomas after two years demonstrated total regression in one patient and significant reduction with thrombosis of the centre of the lesion in another. Homogeneous hyperintensity on T2-W sequences, lack of diffusion restriction and intense contrast enhancement were the hallmarks of cavernous hemangiomas (CSH) in contrast to the other lesions.

**Table 1:** Patient summary shows clinical spectrum in 27 patients.

Patient No.	Age	Sex	Headache	Visual disturbances	Cranial nerve involvement	Surgery	Histopathology
1	57	M	1 month	Blurring	V	Yes	Chordoma
2	34	M	No	Yes	No	Yes	Meningioma
3	17	F	2 months	Blurring	No	Excision	Fungal granuloma
4	23	M	NA	NA	NA	Excision	Dermoid
5	56	F	No	No	No	Partial excision	Pituitary hypophysitis
6	24	M	2 months	No	No	Excision	Meningioma
7	43	M	Yes	Diplopia	III, V, VI	Subtotal	Meningioma
8	40	M	12 months	No	III	Subtotal excision	Schwannoma

9	24	M	1 month	No	No	Near total excision	Schwannoma
10	43	F	NA	NA	NA	ATT	Tuberculosis
11	42	M	11 months	Diminished	V, VII	Subtotal	Schwannoma
12	52	M	1 month	Diminished	II	Subtotal excision	Schwannoma
13	57	F	1 month	Blurring	Tinnitus	Excision	Meningioma
14	34	F	No	Optic Atrophy	No	Excision	Meningioma
15	43	M	No	No	III	Excision	Epidermoid
16	17	M	1 month	No	VI	Subtotal	Cavernous Hemangioma
17	63	M	4 months	Decreased	III, VI	Excision	Meningioma
18	42	F	5 months	Blurring	V	Excision	Schwannoma
19	57	M	Yes	Decreased	No	Subtotal	Pit. Adenoma
20	41	F	NA	Decreased	NA	Excision	Pit. Adenoma
21	43	F	1 week	No	No	Biopsy	Fungal granuloma
22	51	F	12 months	Visual loss	III, IV, VI	Sub total	Hemangioma
23	26	M	2 Years	12 months	VI	Sub total	Hemangioma
24	38	F	Yes	Blurring	No	Biopsy	Hemangioma
25	51	M	4 Years	6 months	VI	Total	Hemangioma
26	13	M	Yes	No	III, VI	Excision	Hemangioma
27	32	F	Yes	Diplopia	V <sub>1,2</sub> , VI Pain 3yrs.	Excision	Fungal granuloma

Note: III, IV, V, VI -- Cranial nerves; NA – Not available; ATT – Antituberculous treatment.

**Table 2:** MRI features of 27 lesions and mean ADC values are shown.

Case No.	T1W	T2W	T2 FLAIR	Post-contrast enhancement	GRE blooming	Extra cavernous sinus extension	Vessel encasement	DWI	Diagnosis	Mean ADC
1	Iso	Iso	Hyper	Homogeneous	No	Yes	No	Restricted	Tuberculosis	0.95
2	Hper	Hypo	Hypo	Rim enhancement	Yes	Yes	No	Restricted	Dermoid	0.068
3	Iso	Iso - Hypo	Iso – Hypo	Homogeneous	Yes	Yes	No	Facilitated	Chordoma	1.13
4	Hypo	Hyper	Hyper	Mild	No	Yes	No	Restricted	Pit. adenoma	0.61
5	Iso	Hypo	Hypo	Homogeneous	No	Yes	No	Restricted	Meningioma	1.64
6	Iso	Hypo	Hypo	Homogeneous	No	Yes	Yes	Facilitated	Aspergilloma	0.84
7	Iso	Iso	Iso	Homogeneous	No	Yes	No	Restricted	Pit. adenoma	1.51
8	Iso	Hyper	Hyper	Intense	Yes	Yes	No	Restricted	Meningioma	1.69
9	Hypo	Hyper	Hyper	Homogeneous	NA	Yes	No	NA	Melanotic Schwannoma	NA
10	Hypo	Hyper	Hyper	Heterogeneous	Yes	Yes	No	Facilitated	Schwannoma	NA
11	Iso	Hyper	Hyper	Homogeneous	Yes	Yes	No	Facilitated	Schwannoma	0.72

12	Hypo	Hyper	Hyper	Homogeneous	No	Yes	No	NA	Schwannoma	NA
13	Hypo	Hyper	Hyper	Heterogeneous	Yes	Yes	Yes	Restricted	Meningioma	1.031
14	Hypo	Iso	Iso	Not Done	No	Yes	Yes	Restricted	Meningioma	0.37
15	Hyper	Hyper	Hyper	Not Done	Yes	Yes	No	Facilitated	Epidermoid	0.656
16	Iso	Iso	Iso	Moderate	NA	Yes	Yes	NA	Meningioma	NA
17	Hypo	Hyper	Hyper	Heterogeneous	Yes	Yes	No	Restricted	Schwannoma	0.485
18	Mixed	Iso	Iso	Heterogeneous	Yes	No	No	Mixed	Pit. adenoma	NA
19	Iso	Iso	Hyper	Minimal	No	Intra-cavernous	Yes	Facilitated	Hemangioma	0.617
20	Hyper	Mild Hyper	Hyper	Homogeneous	No	Yes	Yes	Restricted	Meningioma	NA
21	Iso	Hyper	Hyper	Heterogeneous	No	Yes	Yes (Arteritis)	Facilitated	Fungal granuloma	NA
22	Hypo	Hyper	Hyper	Avid enhancement	No	Yes	Yes	Facilitated	Hemangioma	1.98
23	Hypo	Hyper	Hyper	Avid enhancement	No	Yes	Yes	Facilitated	Hemangioma	1.67
24	Hypo	Hyper	Hyper	Avid enhancement	No	Yes	Yes	Facilitated	Hemangioma	1.18
25	Hypo	Hyper	Not done	Avid enhancement	NA	Yes	Yes	NA	Hemangioma	NA
26	Hypo	Hyper	Hyper	Avid enhancement	NA	Yes	Yes	NA	Hemangioma	NA
27	Iso	Hyper	Hyper	Heterogeneous	No	Yes	Yes	Facilitated	Fungal granuloma	NA

Note: NA – Not available.

**Table 3:** Comparison between diagnoses based on histopathology versus imaging (n=27).

S No.	Lesion	Histopathology	Imaging based diagnosis	Concordance
1	Hemangioma	6	5	85.0%
2	Meningioma	6	2	33.3%
3	Schwannoma	5	2	40.0%
4	Fungal granuloma	3	2	66.6%
5	Pituitary adenoma	2	0	0.0%
6	Epidermoid	1	1	100%
7	Dermoid	1	0	0.0%
8	Tuberculosis	1	0	0.0%
9	Chordoma	1	0	0.0%
10	Pituitary hypophysitis	1	0	0.0%
	Total	27	12	44.4%

## Discussion

### Schwannoma

Trigeminal nerve schwannoma commonly involves the CS and may also arise from other cranial nerves particularly the cranial nerve III. Both trigeminal nerves in the prepontine cistern are symmetrical in course and calibre measuring about 3 to 4 mm in diameter. Fusiform elongation of the trigeminal nerve merging into the tumor indicates origin of the lesion from the V nerve. They follow the expected course of the trigeminal nerve which is best appreciated on FIESTA imaging sequence [2, 3].

Usually the V nerve schwannomas present with slowly progressive hyperesthesia of the face on the side of involvement. Additional neurological symptoms and signs (tinnitus, decreased hearing or hearing loss, facial weakness and visual disturbances) not related to the trigeminal nerve, could be attributed to the location of the tumour. The mandibular branch courses along the inferolateral margin of (not within) the cavernous sinus. Schwannomas arising from this branch can be

confidently diagnosed on the basis of the characteristic extension and expansion through foramen ovale to course through the masticator and prestyloid parapharyngeal space. Resultant atrophy of the muscles of mastication may be seen. One patient in this series presented with facial numbness, difficulty in chewing and absent corneal reflex. These lesions are isointense to hypo intense on T1-W images, mostly hyperintense on T2-W images and show contrast enhancement. Intratumoral haemorrhages and cystic schwannomas have been reported often [4]. Small tumors tend to be homogeneous whereas large ones are frequently heterogeneous in appearance. It was interesting to note that our case series shows one case of bilateral melanocytic schwannoma (Figure 5). Three cases were given radiotherapy in post-operative period. Malignant peripheral nerve sheath tumor may infiltrate the CS. Large tumor size (5 cm), ill-defined infiltrative margins, rapid growth, tumor signal heterogeneity and erosion of the skull base foramina out of proportion to tumor size suggest malignant nature.

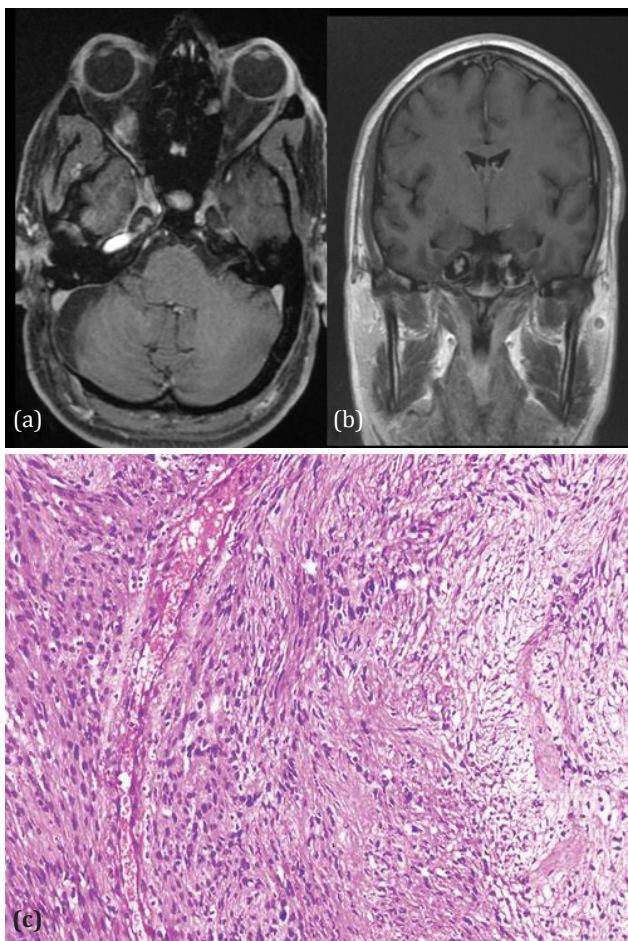


**Figure 5:** (a, b): Gd-DTPA enhanced axial MRI Scan and coronal view show bilateral enhancing schwannomas in the cavernous sinuses. (c) Photomicrograph shows fascicles of spindle-shaped cells arranged compactly (at left) and loosely (at right), with wavy mildly pleomorphic nuclei, inconspicuous nucleoli, and eosinophilic cytoplasm (H-E stain; original magnification,  $\times 100$ ).

## Meningioma

Less frequent sites for Meningioma include the orbit (optic nerve sheath), the paranasal sinus, the choroid plexus and the diploic space of the calvaria. Visual disturbances may range from blurring of vision to hemianopia and only perception of the light. Patients presenting with diplopia also had other cranial nerve involvement (hemifacial numbness, drooping of eyelid). Involvement of the trigeminal nerve, particularly the ophthalmic branch can occur at different locations [5].

One of our patients presented with hemifacial numbness (V1, V2 involvement). Degree of involvement of the cavernous sinus is graded according to a classification system. Category 1 tumours touch or partially encircle the cavernous carotid artery, category 2 tumours completely encircle but do not narrow the lumen of the artery and category 3 tumours encircle and narrow the lumen of the cavernous carotid artery. Category 3 tumours are better recognized by angiography [6]. It is essential to obtain detailed information regarding the tumour and its proximity to the neurovascular bundles by MRI, MR angiography and if necessary DSA of selective internal and external carotid arteries. Venous phase demonstrates the inferior and superior petrosal sinus which might be involved by the lesion. Typically meningiomas show hypointensity with respect to gray matter in all MR imaging sequences and contrast enhancement is avid. Internal carotid artery is often encased and narrowed unlike other tumours (Figure 6). Enhancing dural tail may be seen lining the tentorial edge and reaching the tumor margin. Extension of the tumour may be observed within the prepontine cistern and Meckel cave similar to schwannomas. Ophthalmologic examination 6 months or more after surgery is recommended since the immediate postoperative assessment is not a predictor of long-term recovery of eye motility [7]. Our three patients received external beam radiotherapy following partial resection.

## Cavernous hemangioma

The incidence of cavernous hemangioma in cavernous sinus has a prevalence of 1% with significant female preponderance considered to be due to hormonal influence. The lesion closely mimics other lesions in this region such as meningioma, schwannoma, chordoma, granuloma, lympho-proliferative conditions and carotid aneurysm [8]. MR imaging demonstrates hypointense signal on T1-W and hyperintense signal on T2-W weighted images resembling lesion with high cellular matrix and/or necrotic components [9]. High signal intensity due to T2 prolongation is characteristic of cavernous hemangioma. However, schwannoma of the V

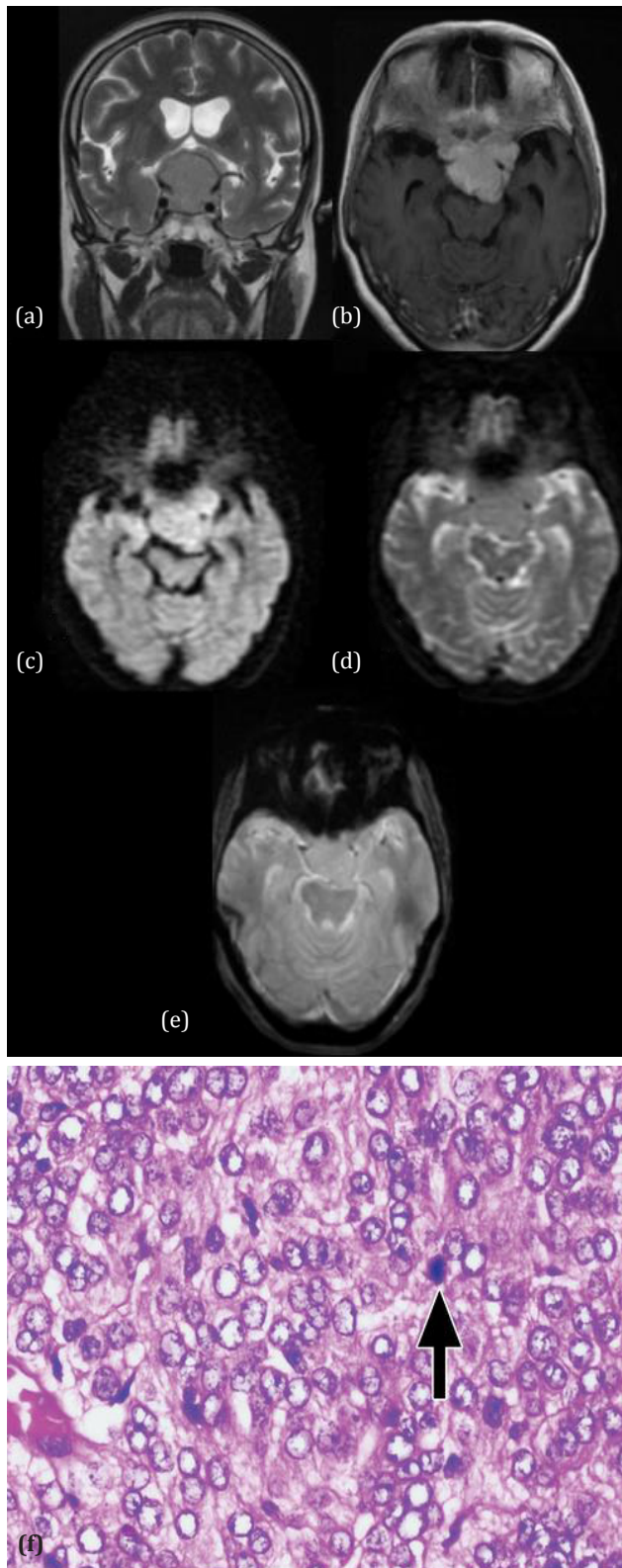


**Figure 6:** MRI Coronal T2W and Gadolinium enhanced (a, b) T1W axial views show large lobulated sellar and suprasellar Meningioma invading the cavernous sinus on both sides. (c, d) DWI reveals restricted diffusion indicating fibrous nature. (e) GRE does not show blooming. (f) Photomicrograph shows sheets of meningothelial cells with mild nuclear pleomorphism, prominent nucleoli, and eosinophilic cytoplasm, as well as a mitotic figure (arrow). Whorling is inconspicuous. The features are those of an atypical meningioma (Hematoxylin-eosin [H-E] stain; original magnification,  $\times 400$ ).

nerve or meningioma remain an important differential diagnosis [10]. Apart from T1 hypointensity and marked T2 and FLAIR hyperintensity, absence of restriction of diffusion was observed in this group of our patients (Figure 7). Intense enhancement of the lesion is a feature unlike the well-known slow and homogeneous delayed enhancement of intra axial cavernous hemangiomas [11]. Lack of restriction on DWI was well exemplified in an earlier report of 15 cavernous hemangiomas by the authors. Blooming is not seen on GRE images. Slow flow and absence of intervening neural/cellular elements outside the vascular channels explains facilitated diffusion in these patients. Recurrent hemorrhages into the wall of the lesion form concentric layers of hemosiderin in the intra-axial cavernous hemangiomas is never appreciated in the lesions of the cavernous sinus. A less aggressive solid/semisolid sclerosing type of cavernous hemangioma is described by Aversa do Souto and Shi et al. [12]. Cavernous sinus hemangiomas respond to radiation unlike the extra axial cavernous angiomas and Gamma Knife surgery is an effective adjuvant treatment modality [13].

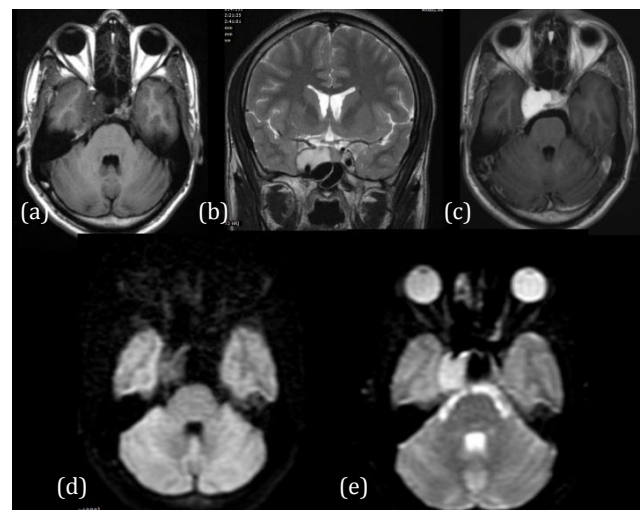


**Figure 7:** Axial T2 FLAIR uniformly hypointense and coronal T2 hyperintense signals (a, b) are noted in the large cavernous hemangioma. (c) Intense Gd-DTPA enhancement of the lesion is appreciated. (d, e) Facilitated diffusion is noted in the DWI images.

### Dermoid cyst

Intracranial dermoid cysts are rare, comprising 0.04-0.7% of all intracranial tumors. They are derived from ectopic epithelial cells that are part of the neural tube, which also explains their typical location close to the midline. Dermoid cysts contain lipid material peripherally and fluid centrally. They may contain hair follicles, sebaceous and sweat glands distinguishing a dermoid from the more common epidermoid cysts. They are very slow-growing and cause focal neurologic signs through encroachment of neurovascular structures.

Spontaneous rupture of intracranial dermoid cysts is a rare phenomenon. Dissemination of keratin and cholesterol breakdown products following rupture may cause a wide variety of symptoms ranging from headache to hallucinations [14]. New onset seizures are typical of ruptured intracranial dermoid cyst. Our patient presented with spontaneous rupture of dermoid cyst causing 2 episodes of new onset seizures since 6 months due to presumed chemical meningitis and chemical irritation. Even though the pathophysiology behind spontaneous rupture is not clearly understood, hypotheses implicated glandular secretions caused by age-dependent hormones as well as head movements and brain pulsations. Dermoid cysts may exhibit mixed densities on CT scan, and rarely enhance following contrast administration.

The intracystic fat and disseminated fat droplets appear hypodense while calcifications in the wall are hyperdense. Hydrocephalus and fat-fluid level may be present following rupture into the ventricular system (Figure 8). A few fat containing pockets / droplets within the subarachnoid spaces were observed in our patient. Dermoid cysts are usually hyperintense on T1-W sequences and variable on T2- W sequences on MRI, although hypointensity on T2-W may be noted due to presence of cholesterol [15]. On DWI the dermoids are hyperintense to brain parenchyma, but demonstrate an ADC that is similar to that of parenchyma and CSF.

### Epidermoid

Intracranial epidermoid cysts also known as congenital cholesteatomas are rare tumors comprising around 0.2 to 1.6 % of all intracranial tumours. Common sites of occurrence are cerebellopontine angle, suprasellar region, quadrigeminal cistern, middle cranial fossa and rarely in the intradiploic space. Cavernous sinus in particular is a very uncommon site to harbor epidermoid cysts [16]. Chemical meningitis and hemorrhage caused by cyst rupture are well described complications of large lesions. T1-W image on MRI demonstrates isointense signals. The lesion is hyperintense on DWI images because of T2 shine-through effect rather than the diffusion restriction, with occasional isointense signals. Wall of the cyst may enhance after Gadodiamide enhancement due to inflammatory reaction or granulation formation around the lesion.

Though the lesion is confused with arachnoid cyst on the conventional spin echo MRI sequences, Fluid Attenuated Inversion Recovery Sequence (FLAIR) distinguishes from the CSF intensity revealing a mildly homogeneous hyperintensity due to ineffective fluid suppression because of the proteinaceous nature of the contents [17]. Epidermoid cysts in the cavernous sinus are classified

into extra cavernous, inter dural and intracavernous types. The extra cavernous type is in the CSF space compressing the cavernous sinus extrinsically. The inter dural lesion is situated between inner and outer layers of the lateral wall of the cavernous sinus while the intracavernous type is exclusively located within the cavernous sinus, a very rare entity. Since epidermoid is a creeping tumour seeking the crevices and corners, resection without damaging adjacent neurovascular structures is challenging specially.

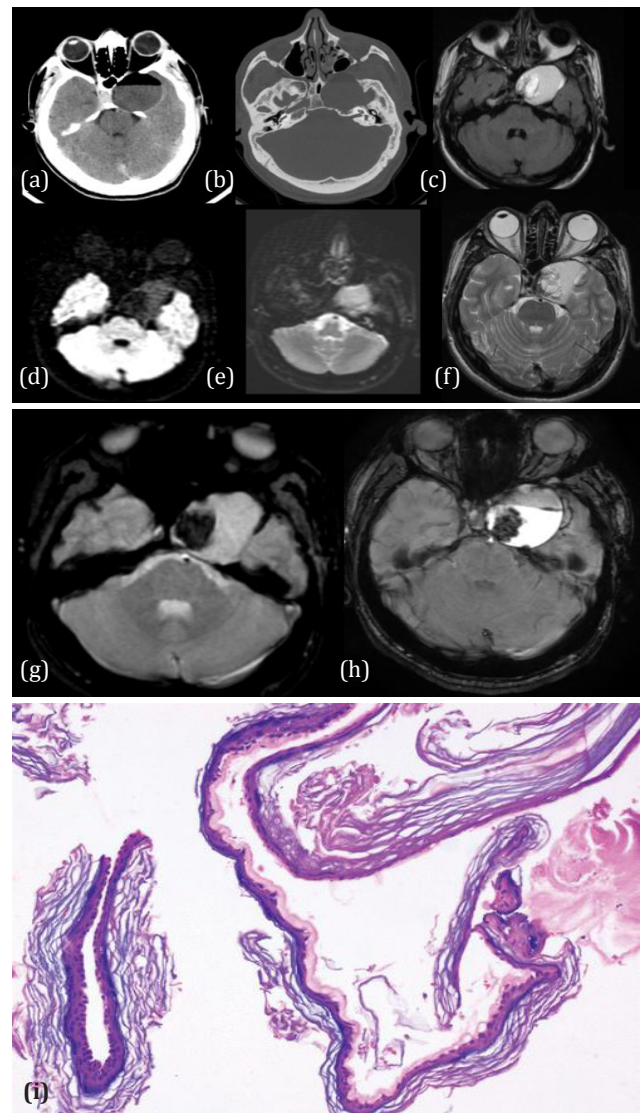


**Figure 8:** CT scan brain (a, b) shows well circumscribed dermoid having a fat-fluid level. (c) Intense enhancement of the lesion is observed on Gd-DTPA injection. (d, e) Facilitated diffusion is appreciated. (f) T2W axial MRI shows mostly hyperintensity with eccentric hypointense signal. (g, h) Eccentric blooming is noted in GRE and SWAN axial images. (i) Photomicrograph shows the cyst wall composed of fibrocollagenous tissue lined by stratified squamous epithelial cells and lamellated keratin. Adnexal structures are not present. (H-E stain; original magnification,  $\times 100$ ).

### Chordoma

Chordomas are rare slow growing malignant

neoplasms arising from remnants of notochord that typically involve the sacrococcygeal region, clivus, or vertebral column, comprising of approximately 1% of intracranial tumors [18]. Approximately 35% to 40% of these tumors occur in the skull base, where they typically involve the clivus. Most commonly, the patient presents with headache, diplopia secondary to VI cranial nerve paresis and visual changes including blurring or sometimes loss of vision. The patient may present with multiple lower cranial nerve palsy symptoms such as facial numbness and asymmetry, dysphagia, hoarseness and speech problems. Large tumors may cause brainstem compression and patients may present with long tract signs and ataxia. Epistaxis and CSF (Cerebrospinal fluid) rhinorrhoea as a rare presentation has also been reported. MRI demonstrates intermediate signal intensity with focal high-signal-intensity on T1-W images representing hemorrhage or high protein (Figure 9). Higher signal intensity on T2-W images is noted. Some hypointensities may represent bony fragments. CT shows bone destruction and calcifications [19]. Histopathological examination of our case showed myxoid matrix without nuclear atypia, infiltrating bone and immunohistochemistry was positive for pancytokeratin and S-100 protein confirming the diagnosis. Recurrence of tumor is well known [20]. Follow up MR imaging done four and half months later showed residual lesion in the Meckel's cave region and left cavernous sinus encasing the carotid.

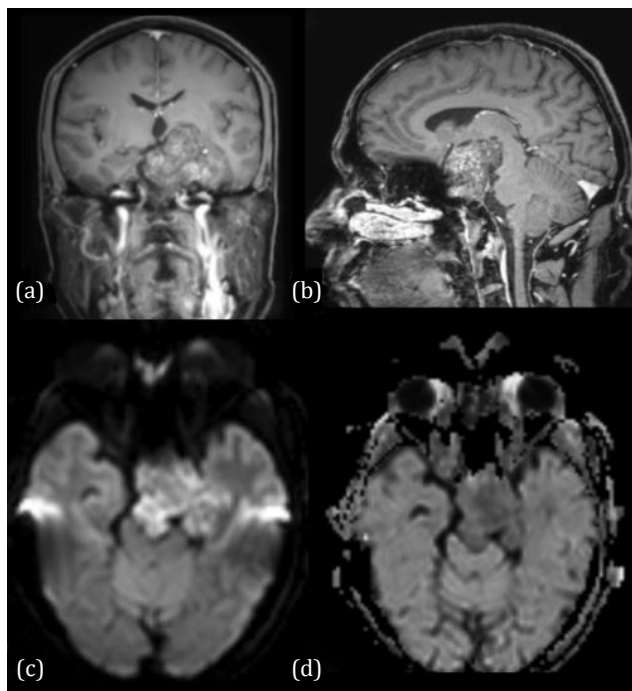


**Figure 9:** MRI Brain coronal and sagittal sections. (a, b) Gd-DTPA enhanced images demonstrate heterogeneous enhancement of the large chordoma with punctate hypointensities suggestive of calcifications. Cavernous sinus and retro sellar extension are noted. Tegmentum is indented. Restricted diffusion (c, d) is observed.

## Pituitary adenoma

Pituitary adenomas are histologically considered as benign tumours. Usually the initial symptoms would be amenorrhea-galactorrhea. Chiasmatic compression, ocular motor signs and epilepsy appear later as tumour grows in size. Six to 10% of pituitary adenomas involve the cavernous sinus and are considered to be invasive [21, 22]. Despite their size and location lateral to the cavernous sinus, the clinical signs of cavernous sinus invasion occur late. Cavernous sinus involvement by pituitary adenoma is uncommon and it makes complete surgical removal difficult. On CT they included cavernous sinus expansion and visible encasement of the internal carotid artery as the criteria. However, the invasive tumor often enhanced to a lesser degree than the cavernous sinuses and ipsilateral internal carotid artery. Histologically only a few patients showed anaplastic features. Intracavernous cranial nerve compression, obliteration, or displacement / invasion of the lateral wall of the cavernous sinus and diffuse bone destruction may be appreciated (Figure 10).

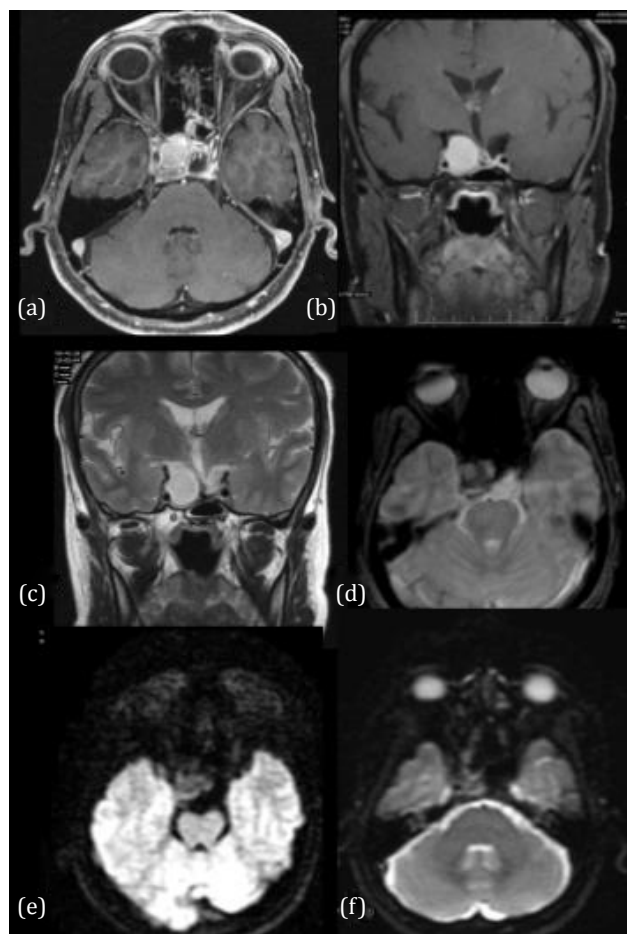


**Figure 10:** (a-f) Pituitary tumour enlarging asymmetrically invading the cavernous sinus.

Total encasement of the intracavernous ICA by the tumor is the most reliable MR imaging sign of cavernous sinus invasion, but this sign occurs very late [23]. The

medial and lateral tangential lines drawn along the intracavernous and supra cavernous ICAs and cross-sectional centers define the four grades of parasellar extension. Often, the diagnosis of invasion remains uncertain until surgery because only direct endoscopic observation allows to distinguish compression from real invasion of the cavernous space.

### Fungal granuloma

Immunocompromised patients may be affected by invasive aspergillosis which extends to the cavernous sinus from the paranasal sinuses as seen in our patient. Ferromagnetic elements, calcium in the fungal hyphae and mucous concretions produce hypointense signal in both T1 and T2 weighted images [24-26]. Intense heterogeneous contrast enhancement is seen. Soft-tissue mass may involve the orbital apex with thickening and displacement of the rectus muscles while involving the adjacent ethmoid sinus. Thrombosis and arterial wall thickening of the cavernous segment of the internal carotid artery may be noted while encasement of its lumen may be noted as seen in our patient though there was no oculomotor involvement or visual disturbances (Figure 11). Seizures in this patient may be due to cortical irritation by the lesion extending outside the confines of the cavernous sinus [27]. Rhinocerebral mucormycosis and actinomycosis spread through the nasal cavity, paranasal sinuses or ear and do not have specific features on MR imaging.

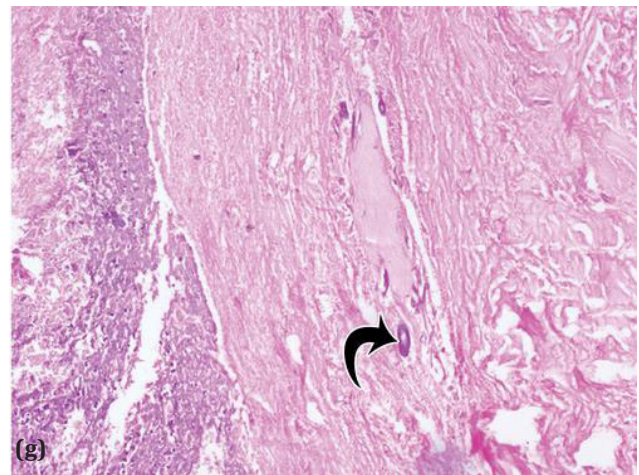
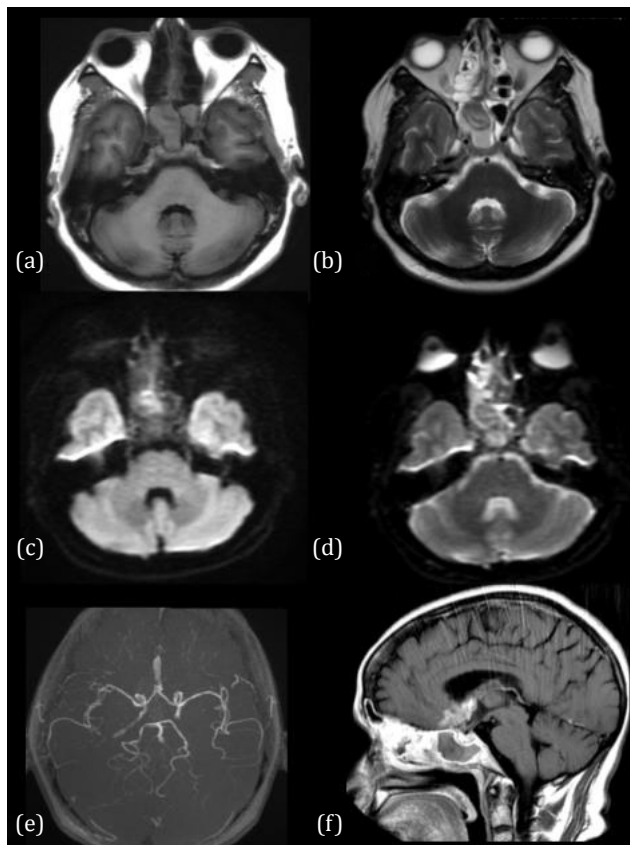


**Figure 11:** T2 FLAIR hypointense and T2W hyperintense (a, b) signals are noted in the suprasellar and sellar regions infiltrating the cavernous sinus on both sides. (c, d) DWI shows facilitated restriction. (e) MR Angiogram shows irregularity and narrowing of the cavernous segment of the internal carotid artery on the right side. (f) Intense enhancement of the aspergillus granuloma shows extension into the cavernous sinus and lamina terminalis in the sagittal view. (g) Photomicrograph shows necrotic debris with occasional broad aseptate basophilic fungal hyphae (arrow). Fungal culture (not shown) grew *Aspergillus flavus* and *Rhizopus arrhizus* (H-E stain; original magnification,  $\times 200$ ).

### Tuberculosis

Tuberculoma in the cavernous sinus is exceptionally rare [28]. The exudates and adhesions compress the cranial nerves in the cavernous sinus. Constitutional symptoms and presence of extracranial tuberculosis lead to a high index of suspicion. Biochemical and CSF culture may be inadequate to arrive at an accurate diagnosis and often necessitates surgery to exclude tumors such as meningioma, lymphoma or metastases [29, 30].

Both T1 and T2 weighted MR images demonstrate iso to hypointense lesion suggestive of a granulomatous process. Therapeutic trial of antituberculous treatment of our patient showed complete regression of the lesion on follow up (Figure 12).

Surgical approach (extradural / trans-cavernous / intradural) depend on the plane of the lesion and its extent. Although radiation therapy is offered, however it can be avoided in infectious / inflammatory lesions therefore, biopsy is often performed to design treatment of choice [6]. Radiographically, on magnetic resonance imaging (MRI), T2 hypointense signal pattern is noted in chronic inflammatory lesions, granulomas and lymphomas. While, cavernomas and hemangiomas demonstrate hyperintensity on T2 sequence; T1 hyperintensity is typically observed in dermoids, adenomas, melanomas and hemorrhagic lesions. Perhaps, radiological identification of the type of lesion may not only help

design appropriate management plan and avoid radiation therapy in selective aetiologies (inflammatory). In the current study, we evaluate the association of findings on MRI with histopathological findings in patients with lesions of the cavernous sinus.

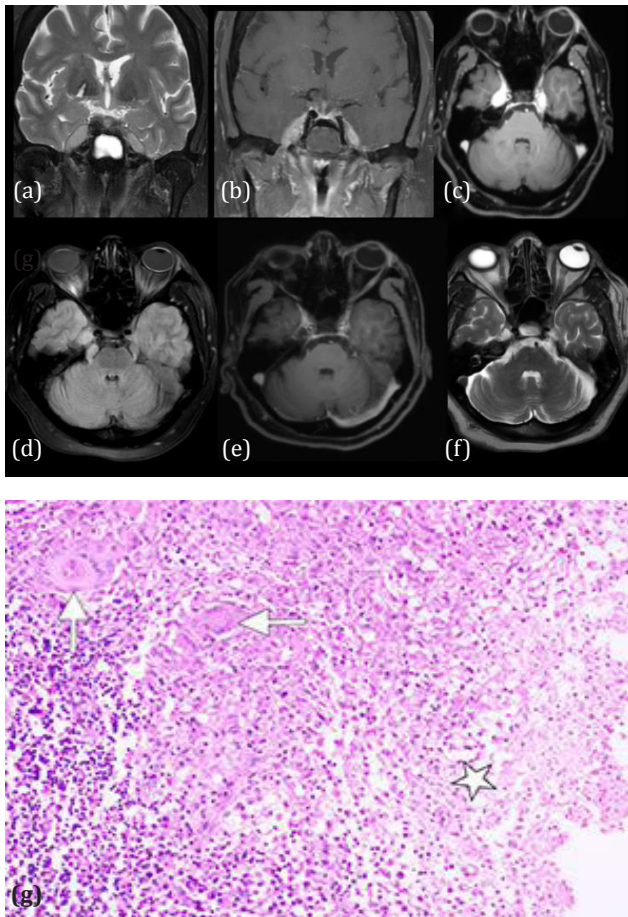


**Figure 12:** (a-f) Coronal T2W image reveals iso to hypointense oblong lesions occupying both cavernous sinuses reaching the lateral walls of the internal carotid arteries. Gd-DTPA enhances both the lesions intensely, treated as tuberculous infection. (d) Axial SPGR sequences demonstrates the lesion involving both the trigeminal nerves. Post antituberculous treatment (e, f) the lesions resolved almost completely. (g) Photomicrograph shows necrotizing granulomatous inflammation—discrete and confluent granulomas composed of epithelioid histiocytes and multinucleate giant cells (arrows). Areas of necrosis (☆) are also depicted (H-E stain; original magnification,  $\times 100$ ).

The current study evaluated the role of imaging in clinical diagnosis and decision making of lesions affecting cavernous sinus. Although a few conditions (hemangiomas and fungal granulomas) have characteristic findings on imaging that can help in diagnosis; more often than not, the diagnosis and management plan is predominantly based on histopathology. Importantly, in two-third of patients with fungal granuloma, imaging is helpful in accurate diagnosis, perhaps avoiding the need for radiation therapy in these patients.

In most of the patients in the current study, schwannomas are isointense to hypo intense on T1-W images, mostly hyperintense on T2-W images and show contrast enhancement. Three patients were advised radiotherapy in post-operative period. Whereas, meningiomas, typically show hypointensity with respect to gray matter in all MR imaging sequences and contrast enhancement is avid. Internal carotid artery is often encased and narrowed unlike other tumours. Extension of the tumour may be observed within the prepontine cistern and Meckel cave similar to schwannomas. However, in the current study, except for extra cavernous extension seen in all of them, there was no noticeable pattern on T1, T2, T2 flair or post-contrast enhancement.

In cavernous hemangiomas, MR imaging demonstrates hypointense signal on T1-W and hyperintense signal on T2-W weighted images resembling lesion with high cellular matrix and/or necrotic components. Infact, high signal intensity due to T2 prolongation is characteristic of cavernous hemangioma. However, schwannoma of the V nerve or meningioma remain an important differential diagnosis. Apart from T1 hypointensity and marked T2 and FLAIR hyperintensity, absence of restriction of diffusion was observed in all our patients. While blooming is not seen on GRE images; slow flow and absence of intervening neural/cellular elements outside the vascular channels explains facilitated diffusion in these patients.

Dermoid cysts are usually hyperintense on T1-W sequences and variable on T2- W sequences, but the hypointensity on T1 images in our patient with dermoid cyst may be due to intra-cystic fat and disseminated fat droplets. On the other hand, although epidermoid lesions of cavernous sinus demonstrate iso-intense signals on T1-W image, the lesion in our patient was hyperintense on T1, T2 and T2 FLAIR probably because of T2 shine-through effect, with occasional isointense signals. Wall of the cyst may have enhanced with Gadodiamide due to inflammatory reaction or granulation formation around the lesion. In the single patient with chordoma in the current series, MRI demonstrated intermediate signal intensity T1-W images suggesting haemorrhage or high protein and a higher signal intensity on T2-W images. Recurrence of chordoma is well known and follow up MR imaging done four and half months later showed residual lesion in the Meckel's cave region and left cavernous sinus encasing the carotid.

In pituitary adenomas, the invasive tumor often enhanced to a lesser degree than the cavernous sinuses and ipsilateral internal carotid artery. Total encasement of the intracavernous ICA, observed in both the patients in the current series, is the most reliable MR imaging

sign of cavernous sinus invasion, but this sign occurs very late. Often, the diagnosis of invasion remains uncertain until surgery because only direct endoscopic observation allows to distinguish compression from real invasion of the cavernous space (Figure 13).

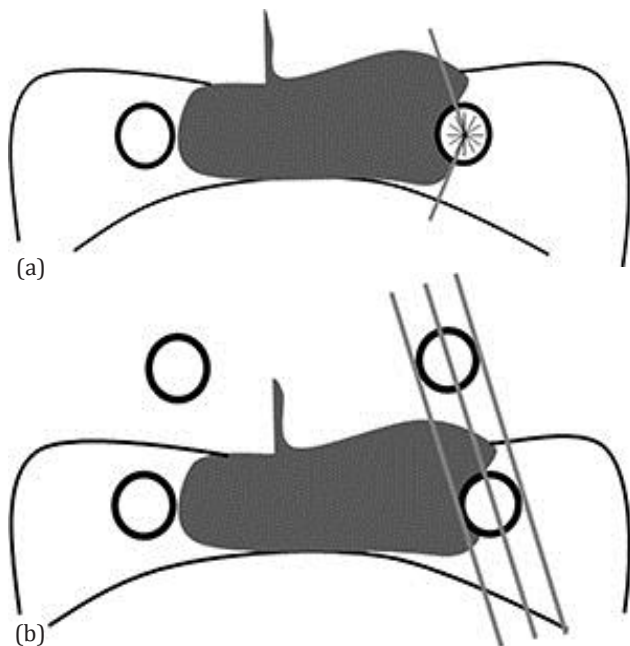


**Figure 13:** (a) Schematic diagram of the system of Knosp et al (30) for classifying cavernous sinus invasion by pituitary adenomas. Three lines are drawn on a coronal section through the sella: a medial tangent to the cavernous and supraclinoid parts of the ICA, an intercarotid line bisecting the cross-sectional lumen of the cavernous and supraclinoid parts of the ICA, and a lateral tangent to the cavernous and supraclinoid parts of the ICA. Lesions are classified as grade 0: the lesion (pituitary adenoma) does not cross the medial tangent; grade 1: the lesion crosses the medial tangent but not the intercarotid line; grade 2: the lesion crosses the intercarotid line but not the lateral tangent; or grade 3: the lesion crosses the lateral tangent. In the example represented, the lesion is crossing the intercarotid line but not the lateral tangent (grade 2). Grades 2 and 3 strongly predict cavernous sinus invasion. (b) Schematic diagram of the system of Cottier et al (31) for calculating the percentage of the circumference of the ICA that is in contact with the pituitary adenoma invading the cavernous sinus. The circular perimeter of the cavernous segment of the ICA is divided into 12 clock hours, and the number of clock hours in contact with the tumor is calculated and divided by 12. Greater than 67% (>8/12 clock hours) circumferential contact strongly predicts cavernous sinus invasion, and less than 25% (<3/12 clock hours) circumferential contact predicts the absence of cavernous sinus invasion. In the illustrated example, the lesion is in contact with four of 12 clock hours, which is equal to 33% circumferential contact.

Invasive fungal granuloma like aspergillosis which extends to the cavernous sinus is often seen in immunocompromised. Our findings of hypointense signals in T1 and T2 images with heterogenous contrast enhancement may be due to ferromagnetic elements, calcium in the fungal hyphae and mucous concretions, reported previously by Chandra et al. The encasement

seen in one of our patients may be due to thrombosis and arterial wall thickening of the cavernous segment of the internal carotid artery.

Similarly, the iso to hypointense signal both on T1 and T2 weighted MR images was suggestive of a granulomatous lesion, with a probability of tuberculosis. Therefore, after informed consent from the patients, a therapeutic trial of antituberculous treatment resulted in complete regression of the lesion on follow up, thus helping us avoid probable biopsy and/or radiation therapy.

### Acknowledgements

Acknowledgement to the source of the figures (Mahalingam HV et al., <https://doi.org/10.1148/rj.2019180122>).

### Conflicts of interest

Authors declare no conflicts of interest.

### References

- [1] Razek AAKA, Castillo M. Imaging lesions of the cavernous sinus. *AJNR Am J Neuroradiol.* 2009; 30(3):444–452.
- [2] Majoie C, Hulsmans F, Castelijns J, Sie LH, Walter A, et al. Primary nerve-sheath tumors of the trigeminal nerve: clinical and MR findings. *Neuroradiology.* 1999; 41(2):100–108.
- [3] Lo P, Harper C. Intracavernous schwannoma of the abducens nerve: A review of the clinical features, radiology and pathology of an unusual case. *J Clin Neurosci.* 2001; 8(4):357–360.
- [4] Skolnik AD, Loevner LA, Sampathu DM, Newman JG, Lee JY, et al. Cranial nerve schwannomas: diagnostic imaging approach. *Radiographics.* 2016; 36(5):1463–1477.
- [5] Hirsch WL, Sekhar LN, Lanzino G, Newman JG, Lee JY, et al. Meningiomas involving the cavernous sinus: value of imaging for predicting surgical Complications. *AJR* 1993; 160(5):1083–1088.
- [6] Marc Sindou, Mustapha Nebbal, Bulent Guclu. Cavernous sinus meningiomas: imaging and surgical strategy neurosurgery. In: *advances and technical standards in neurosurgery* 2014; 42:103–121.
- [7] Sekhar LN, Altschuler E. Meningiomas of the cavernous sinus. In: Al Mefti O, ed. *Meningiomas.* New York, Raven Press Ltd. 1991; pp.445–460.
- [8] Yadav RR, Boruah DK, Yadav G, Pandey R, Phadke RV. Imaging characteristics of cavernous sinus cavernous hemangiomas. *Neuroradiol J.* 2012; 25(5):515–524.
- [9] Mahajan A, Rao VRK, Anantaram G, Polnaya AM, Desai S, Desai P, Vadapalli R, Panigrahi M. Clinical-radiological-pathological correlation of cavernous sinus hemangioma: Incremental value of diffusion-weighted imaging. *World J Radiol.* 2017; 9(8):330–338.
- [10] Yao Z, Feng X, Chen X, Zee C. Magnetic resonance imaging characteristics with pathological correlation of cavernous malformation in cavernous sinus. *J Comput Assist Tomogr.* 2006; 30:975–979.
- [11] Jinhu Y, Jianping D, Xin L, Yuanli Z. Dynamic enhancement features of cavernous sinus cavernous hemangiomas on conventional contrast-enhanced MR imaging. *AJNR Am J Neuroradiol.* 2008; 29(3):577–581.
- [12] Souto AA, Marcondes J, Silva M R, Chimelli L. Sclerosing cavernous hemangioma in the cavernous sinus: Case report. *Skull Base.* 2003; 13(2):93–99.
- [13] Wang Y, Li P, Zhang XJ, Xu YY, Wang W. gamma knife surgery for cavernous sinus hemangioma: A report of 32 cases. *World Neurosurg.* 2016; 94:18–25.
- [14] Dange N, Mahore A, Goel A. Ruptured giant dermoid cyst of the cavernous sinus. *J Clin Neurosci.* 2010; 17(8):1056–1058.
- [15] Muçaj S, Sahin M, Ugurel , Dedushi K, Ramadanani N, et al. Role of MRI in diagnosis of ruptured intracranial dermoid cyst. *Acta Inform Med.* 2017; 25(2):141–144.
- [16] Gharabaghi A, Koerbel A, Samii A, Safavi-Abbasi S, Tatagiba M, et al. Epidermoid cysts of the cavernous sinus. *Surg Neurol.* 2005; 64(5):428–433.
- [17] Melhem ER, Jara H, Eustace S. Fluid-attenuated inversion recovery MR imaging: identification of protein concentration thresholds for CSF hyperintensity. *AJR Am J Roentgenol.* 1997; 169(3):859–862.

- 
- [18] Prashant SATHE, Amit M, Aadil C. Cystic chordoma of the cavernous sinus. *Turk Neurosurgery*. 2019; 29(2):300–302.
- [19] Erdem E, Angtuaco EC, Hemert RV, Park JS, Al-Mefty O. Comprehensive review of intracranial chordoma. *RadioGraphics*. 2003; 23(4):995–1009.
- [20] Fischbein NJ, Kaplan MJ, Holliday RA, Dillon WP. Recurrence of clival chordoma along the surgical pathway. *AJNR Am J Neuroradiol*. 2000; 21(3):578–583.
- [21] Cottier JP, Destrieux C, Brunereau L, Bertrand P, Moreau L, et al. Cavernous sinus invasion by pituitary adenoma: MR imaging. *Radiology*. 2000; 215(2):463–469.
- [22] Connor SE, Wilson F, Hogarth K. Magnetic resonance imaging criteria to predict complete excision of parasellar pituitary macroadenoma on postoperative imaging. *J Neurol Surg, Part B Skull Base*. 2014; 75(1):41–46.
- [23] Micko SG, Wöhrer A, Wolfsberger S, Knosp E. Invasion of the cavernous sinus space in pituitary adenomas: endoscopic verification and its correlation with an MRI-based classification Alexander *J Neurosurg*. 2015; 122(4):803–811.
- [24] Aribandi M, McCoy V, Bazan C. Imaging features of invasive and noninvasive fungal sinusitis: a review. *Radiographics*. 2007; 27(5):1283–1296.
- [25] Stringer SP, Ryan MW. Chronic invasive fungal rhinosinusitis. *Otolaryngol Clin North Am*. 2000; 33(2):375–387.
- [26] Chandra S, Goyal M, Mishra NK, Gaikwad SB. Invasive aspergillosis presenting as a cavernous sinus mass in immunocompetent individuals; report of 3 cases. *Neuroradiology*. 2000; 42(2):108–111.
- [27] Ohta S, Nishizawa S, Namba H, Sugimura H. Bilateral cavernous sinus actinomycosis resulting in painful ophthalmoplegia: Case report. *J Neurosurg*. 2002; 96(3):600–602.
- [28] Morgado C, Ruivo N. Imaging meningo-encephalic tuberculosis. *Eur J Radiol*. 2005; 55(2):188–192.
- [29] Rebai R, Boudawara MZ, Bahloul K, Chabchoub I, Chaari S, et al. Cavernous sinus tuberculoma: diagnostic difficulties in a personal case. *Surg Neurol*. 2001; 55(6):372–375.
- [30] Jaimovich SG, Thea VC, Guevara M, Gardella JL. Cavernous sinus tuberculoma mimicking a neoplasm: Case report, literature review, and diagnostic and treatment suggestions for tuberculomas in rare locations. *Surg Neurol Int*. 2013; 4:158.